1 Experimental

Materials

Zirconium (IV) chloride (>99.5%, $ZrCl_4$, Sigma Aldrich), 4,4'-stilbenedicarboxylic acid (98%, $C_{16}H_{12}O_4$, ABCR), acetic acid (99%, CH_3COOH, Sigma Aldrich), N,N-dimethylformamide (99%, DMF, Sigma Aldrich), 4-nitrobenzoic acid (98 %, $C_7H_5NO_4$, Aldrich), D-glucose (>99%, $C_6H_{17}O_6$, AppliChem), sodium sulfide nonahydrate ($Na_2S\ 9{\cdot}H_2O$), sulfuric acid (≥95 %, H_2SO_4, fisher), nitric acid (70 %, HNO_3, Sigma Aldrich), sodium hydroxide (>97 %, NaOH, VWR) were used as obtained.

Linker synthesis of 4,4'-azostilbenedicarboxylic acid (H_2*abdc*)

The linker H_2*abdc* was synthesized according to literature procedures.[1]

MOF synthesis

Synthesis of UiO-*abdc*

The synthesis of the UiO-*abdc* was performed as described in literature.[2]

Synthesis of MIL-140D-*sdc* and MIL-140D-*H*

All MOF syntheses were conducted in round bottom flasks. In the general synthesis procedure $ZrCl_4$ (1 eq) and the linker (1 eq) were dissolved in a mixture of DMF and acetic acid as modulator. The reaction mixture was heated up to 190 °C for 24 hours. After the flasks were cooled down to room temperature, the resulting product was separated by centrifugation. The solid was washed once with DMF and acetone. The obtained solids were dried in air at 120 °C overnight.

Table S1: Synthesis parameters for the preparation of MIL-140D-*sdc* and MIL-140D-H.

	n(Linker, $ZrCl_4$) / mmol	V(DMF) / mL	n(DMF) / mmol	n(acetic acid) / mmol
MIL-140D-*sdc*	5.20	40	519.80	12.91
MIL-140D-*H*	1.29	8	129.14	12.91

Synthesis of functionalized MIL-140D-*sdc* frameworks via SALE

All SALEs were performed in 25 mL Pyrex glass vessels. In the general synthesis procedure MIL-140D-*sdc* (1 eq) and the new linker H_2*abdc* (0.2 – 1 eq) were dissolved in a DMF (125 eq). The reaction mixture was heated up to 120 °C for one day. After the vessels were cooled down to room temperature, the resulting product was separated from the liquid phase by centrifugation. The solid was washed with DMF until the red color of the solution disappears and once with acetone. The obtained solids were dried in air at 120 °C overnight.

Table S2: Synthesis parameters for the SALE with MIL-140D-*sdc* and H_2*abdc* as new linker molecule.

H_2*abdc* / eq	H_2*abdc* / mmol	V(DMF) / mL	n(MIL-140D-*sdc*) / mmol
0.2	0.17	8	0.83
0.4	0.26	8	0.83
0.6	0.39	8	0.83
0.8	0.66	8	0.83
1.0	0.83	8	0.83

Incorporation of Cupper

For the incorporation of Cu^{2+} into the MIL-140D-*sdc*/*abdc* frameworks 0.83 mmol of the raw material was dissolved in 5 mL DMF. Afterwards, $CuCl_2$ 2 H_2O (0.2 – 1 eq) was added to the suspension followed by 2 min step of ultra sonification. After stirring for 1 h at room temperature, the sample was centrifuged and washed with DMF until the color of the solution disappears and once with acetone. The solids were dried at 120 °C over night.

Table S3: Synthesis parameters for the incorporation of Cu^{2+} into the MIL-140D-*sdc*/*abdc* samples.

$CuCl_2$ 2 H_2O / eq	m($CuCl_2$ 2 H_2O) / mg
0.2	28.1
0.4	43.9
0.6	65.9
0.8	112.68
1.0	140.81

For the incorporation of Cu^{2+} into the MIL-140D-*H* and the UiO-*abdc* frameworks 0.53 and 0.02 mmol of the raw material was dissolved in 5 mL DMF. Afterwards, the same amount of $CuCl_2$ 2 H_2O was added to the suspension followed by 2 min step of ultra sonification. After stirring for 1 h at room temperature, the sample was centrifuged and washed with DMF until the color of the solution disappears and once with acetone. The solids were dried at 120 °C over night.

Reaction with H_2S

The reaction of the Cu^{2+} incorporated samples was conducted in beakers. The material to be flushed was placed there. The Na_2S 9 H_2O (0.1 mmol for 100 ppm) was weighed in a snap-on lid glass and also placed in it. For the gas evolution 0.4 mL H_2SO_4 were added and the beaker was covered. After 5 minutes the reaction was stopped and the MOF was recovered.

For the *in-situ* UV/Vis measurement of the Cu^{2+} loaded samples a 100 ppm H_2S test gas cylinder was used.

Characterization methods

Powder X-ray diffraction: PXRD was carried out in transmission mode using a Stoe Stadi P diffractometer operated with Ge(111)-monochromatized $CuK_{\alpha 1}$ radiation (λ = 1.54060 Å) and a linear position sensitive detector with scintillation counter.

Thermogravimetric analyses: TGA were performed using a Netzsch STA 409PC thermoanalyzer. For this purpose, the samples were filled into alumina crucibles and heated under a flow of air at a heating rate of 5 °C min^{-1} up to 1000 °C.

Physisorption measurements: Argon physisorption isotherms were measured at 87 K using a Quantachrome Autosorb-1 instrument. Nitrogen physisorption isotherms were measured at 77 K using a Quantachrome Autosorb-3 instrument The samples were solvent-exchanged with acetone using a Soxhlet extractor and outgassed at 120 °C in vacuum using the Quantachrome Autosorb-1 instrument immediately prior to the measurement.
The ‘‘Micropore BET Assistant’’ implemented in the ASiQwin 2.0 software from Quantachrome was used to determine the maximum relative pressure for the BET (Brunauer, Emmett, Teller) plot. It determines the BET range according to the theory of Rouquerol, which was shown to be appropriate for the comparison of different MOFs.

IR-Spectroscopy: IR spectra were measured using a Tensor 27 FT-IR-spectrometer and the ATR method. The MOF samples were solvent-exchanged with acetone and dried at 120 °C.

Energy-dispersive X-ray spectroscopy: EDX spectra were measured with a JSM-6610 SEM with an integrated EDX-detector XFlash Detector 410-M using a beam energy of 15 kV. Samples were dispersed in ethanol and drop-casted on polished graphite supports.

Raman-Spectroscopy: Raman spectra were measured a Senterra microscope (Bruker). The used laser has a wavelength of 532 nm with a power of 2 mW and a resolution of 3-5 cm^{-1}. The integration time was 5 s and two loops were performed per measuring point.

^{1}H-NMR-Spectroscopy: For the characterization with ^{1}H-NMR spectroscopy, the MOFs (10 mg) were disassembled in DMSO-*d*6 (0.6 mL) through the addition of HF (15 µL, 48 wt%) and stirred for 24 h. Then $CaCl_2$ was added and the suspension was decanted after a short period of time.

UV/Vis Spectroscopy: The samples were measured as powder via UV/Vis spectroscopy with a Praying Mantis device (Cary 4000, Agilent Technologies) and a gas measurement chamber.[3] Depending on the method, the samples were measured after the exposure to H_2S or *in-situ* using a cycled measurement.

Characterization

Structure of MIL-140D-*sdc* and MIL-140D-*abdc*[4,5]

The crystal structure of MIL-140D-*sdc* consists of infinite one-dimensional zirconium oxide chains as IBUs which are oriented parallelly along the *c*-axis. The coordination number of the zirconium cations is seven, due to a coordination by three μ_3-O^{2-} oxygen ions and four oxygen ions from the carboxylate groups. For this reason, the crystallographic parameter for the *c*-axis is very similar for all compounds of the MIL-140 series. One IBU chain is connected via the 4,4'-stilbene dicarboxylic acid (H_2*sdc*) to six other chains stretching a three-dimensional framework with the sum formula [ZrO(sdc)]. The resulting one-dimensional pores are located between three zirconium oxide chains and are framed by the linkers. The crystal structure of MIL-140D-*abdc* is similar to that of MIL-140D-*sdc*. Here, only a linker with an azo group was integrated (4,4'-azostilbene dicarboxylic acid).

A special feature of this structure is the linker geometry. Although only one linker molecule is used, it has two different environments. The distribution is 50% each and differs in the distance and orientation to the neighbouring linker molecule. The linker molecules arranged parallelly along the *a*-axis show a distance of about 3.5-4.5 Å, whereas the links across the *a*- and *b*-axis have a distance of 7-8 Å to each other.

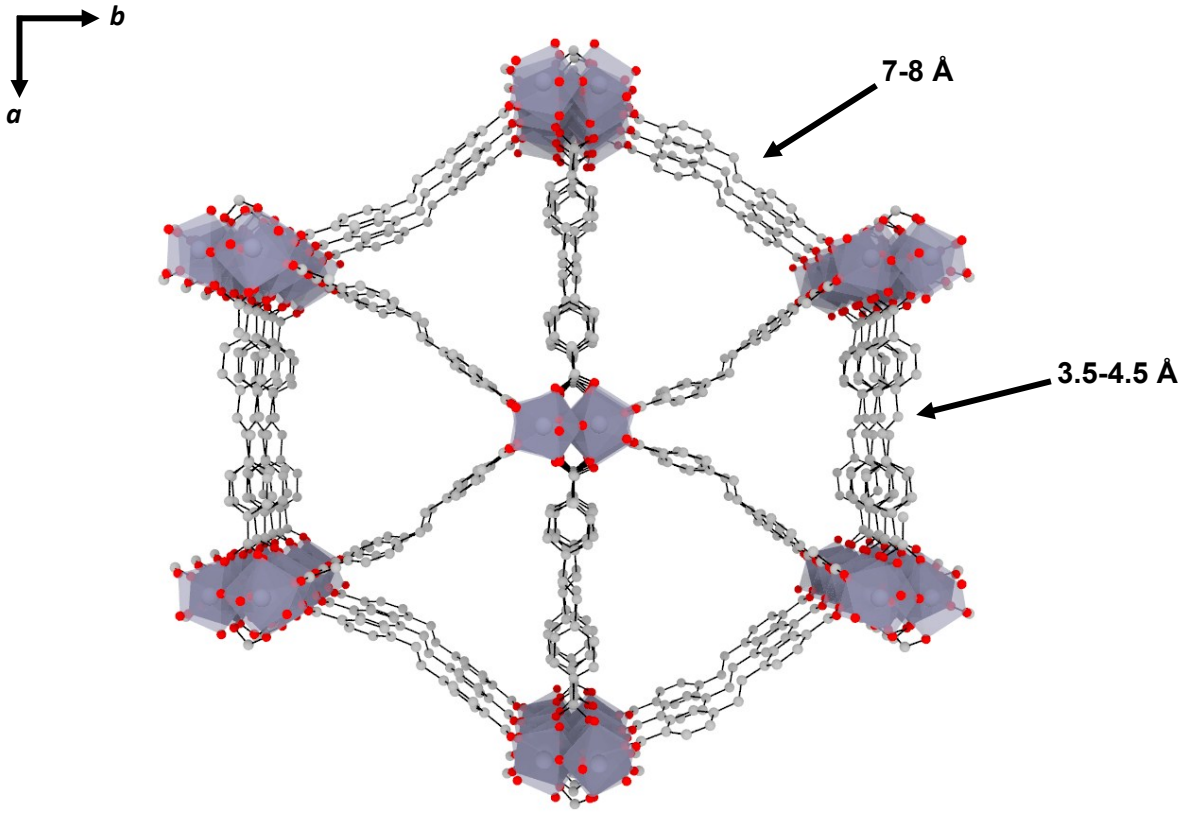

Figure S1: Crystal structure of MIL-140D-*sdc* with view along the *c*-axis with 4,4'-stilbene dicarboxylic acid as linker molecule (zirconium: purple, oxygen: red, carbon: grey, hydrogen atoms are missing for reasons of clarity).

[1]H-NMR spectroscopy

For the analysis of the [1]H-NMR spectra the C-C double bond (2 H) of the H_2*sdc* was used as reference and its integral was set to 2. From the combined intensities of the aromatic protons H_2*sdc*, *trans*-H_2*abdc* and *cis*-H_2*abdc* (see figure S1), the ratios between the two linkers could be calculated (see table S4).

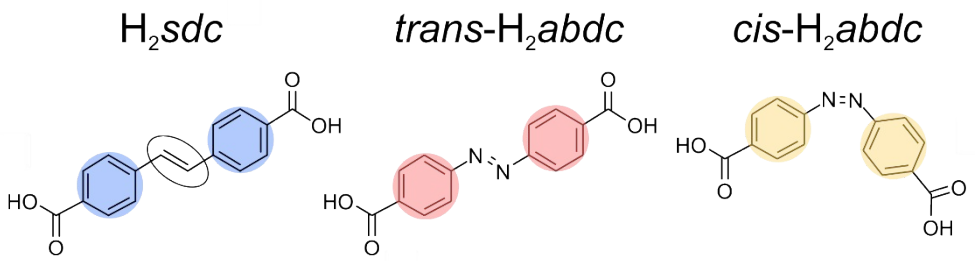

Figure S2: Illustration of the linker molecules. The aromatic protons are highlighted in different colors to simplify recognition in the following [1]H-NMR spectra.

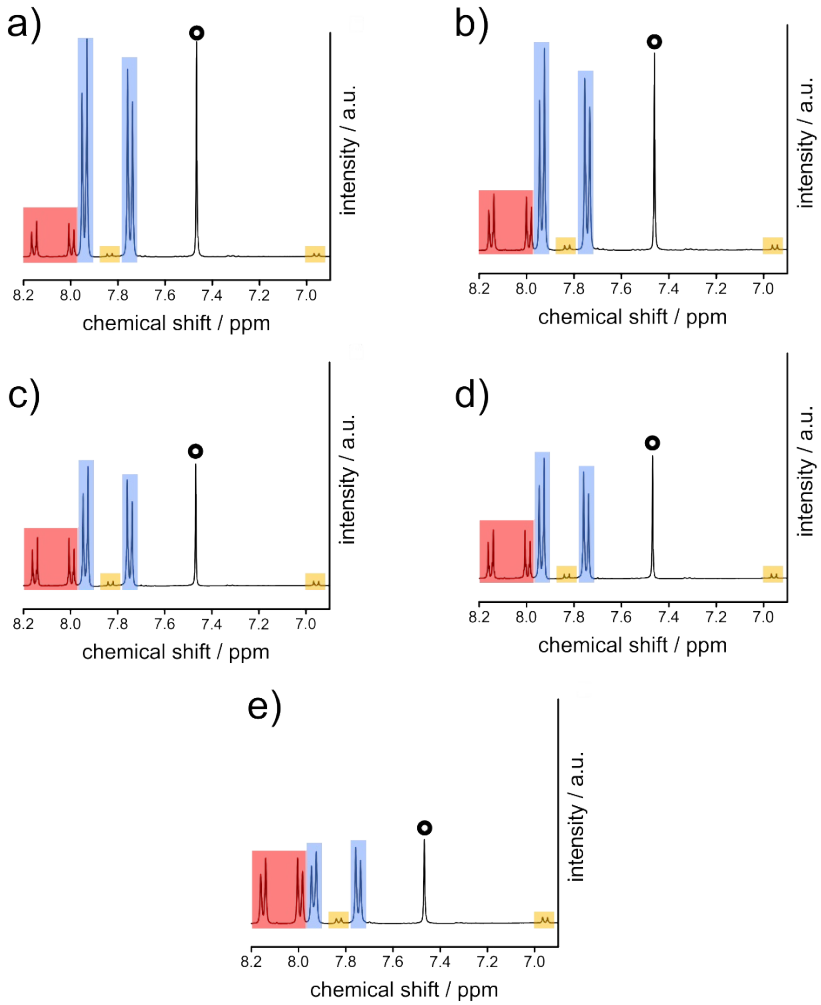

Figure S3: [1]H-NMR spectra in DMSO-*d*6 of the disassembled MIL-140D-*sdc* after the SALE with a) 0.2 eq H_2*abdc*, b) 0.4 eq H_2*abdc*, c) 0.6 eq H_2*abdc*, d) 0.8 eq H_2*abdc* and e) 1.0 eq H_2*abdc*. The C-C double bond of the H_2*sdc* is marked with a circle and used as reference. The observed signals of the aromatic protons are marked in blue (H_2*sdc*), red (*trans*-H_2*abdc*) and yellow (*cis*-H_2*abdc*).

Table S4: Calculation of the conversion of the Sale of MIL-140D-*sdc* with different amounts of H_2*abdc*.

Amount of linker / eq	$I(H_2abdc_{trans})$	$I(H_2abdc_{cis})$	$I(H_2sdc)$	I_{ges}	Conversion / %
0.2	1.26	0.23	8.50	9.99	14.9
0.4	2.08	0.31	8.51	10.9	21.9
0.6	3.05	0.50	8.36	11.91	29.8
0.8	5.43	0.73	8.52	14.68	41.9
1.0	6.71	0.84	8.37	15.92	47.4

Powder X-ray diffraction

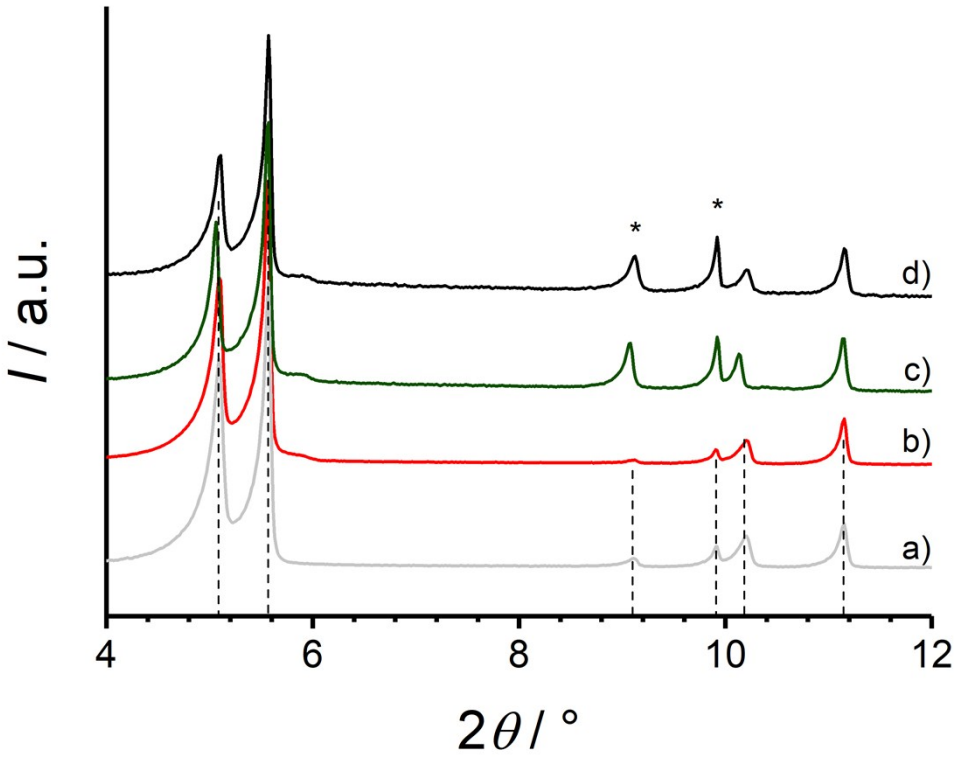

Figure S4: Powder XRD pattern of a) MIL-140D-*sdc* as prepared, b) of MIL-140D-*sdc*/*abdc* after the SALE with 1 eq H_2*abdc*, c) of the same MOF after the incorporation of 1 eq Cu^{2+}, d) after the exposure to 100 ppm H_2S. The dotted lines indicate the reflections peaks of the simulated MIL-140D-*sdc*[4] and the asterisks the reflections with increasing intensity.

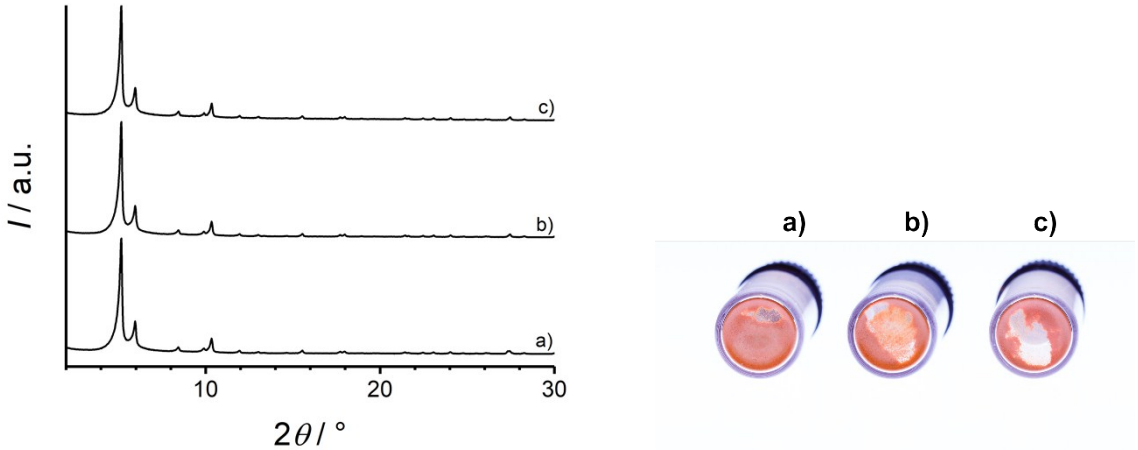

Figure S5: Left: Powder XRD pattern of the UiO-*abdc*: a) as prepared, b) after attempted incorporation of Cu^{2+} and c) after exposure to H_2S. Right: photographs of the UiO-*abdc* in the same order.

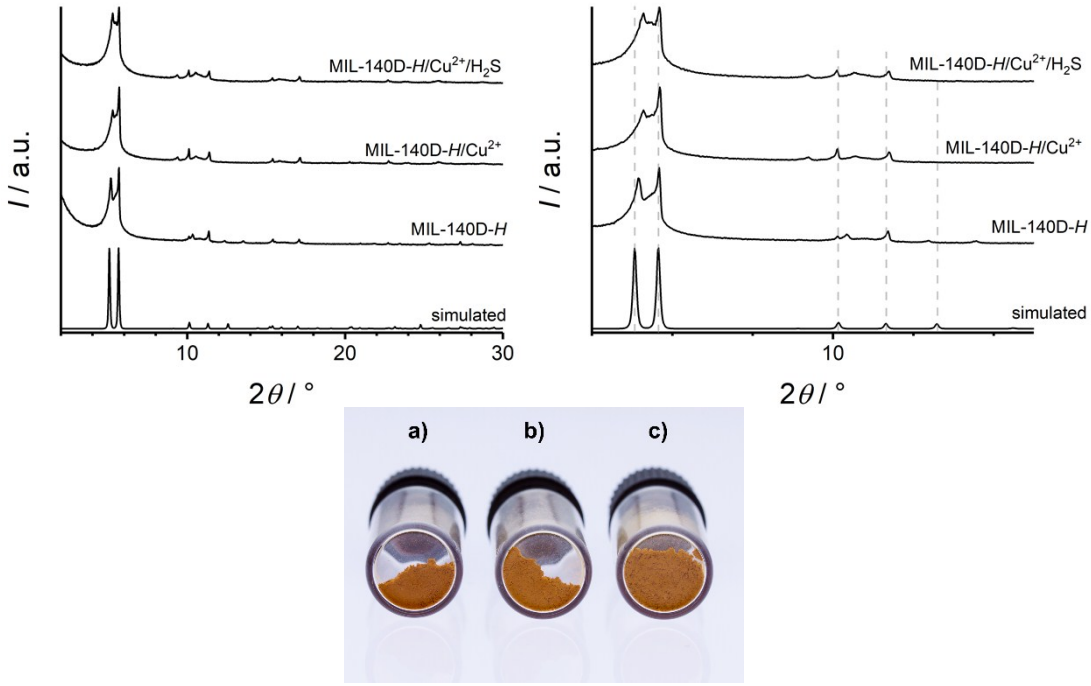

Figure S6: Top left: Simulated powder XRD pattern of the MIL-140D-*H*[5] and the prepared samples MIL-140D-*H* (as prepared), MIL-140D-*H*/Cu^{2+} (after attempted incorporation of Cu^{2+}) and MIL-140D-*H*/Cu^{2+}/H_2S (after exposure to H_2S). Top right: Bottom: Zoomed section of the simulated powder XRD pattern of the MIL-140D-*H*[5] and the prepared samples MIL-140D-*H* (as prepared), MIL-140D-*H*/Cu^{2+} (after attempted incorporation of Cu^{2+}) and MIL-140D-*H*/Cu^{2+}/H_2S (after exposure to H_2S). Photographs of the MIL-140D-*H*: a) as prepared, b) after attempted incorporation of Cu^{2+} and c) after exposure to H_2S.

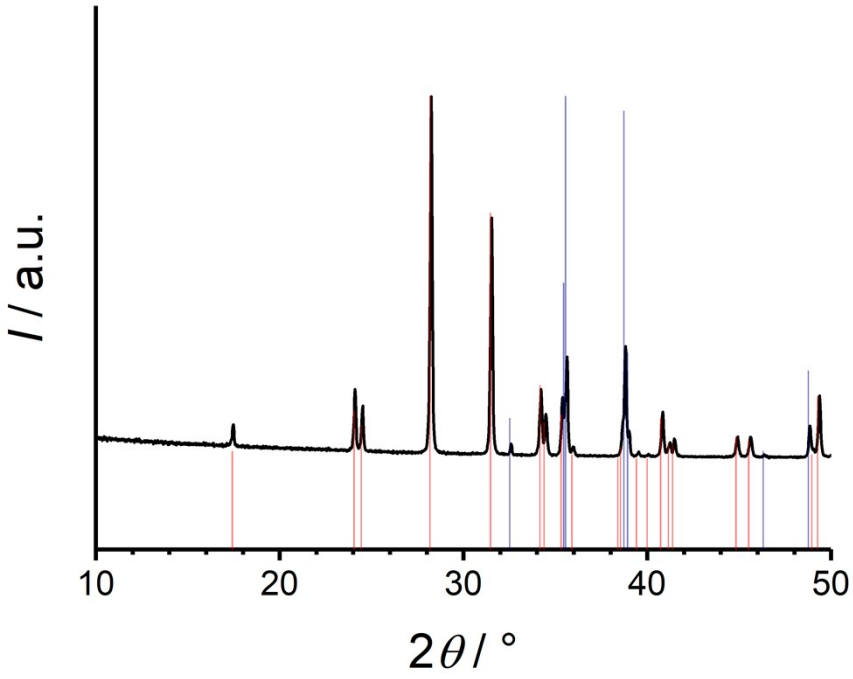

Figure S7: Powder XRD pattern of the residue after a thermogravimetric analysis of the MIL-140D-*sdc*/*abdc* sample prepared with 1 eq H_2*abdc* and 1 eq $CuCl_2$ 2 H_2O. The red lines represent the XRD pattern of ZrO_2 and the blue lines represent that of CuO.

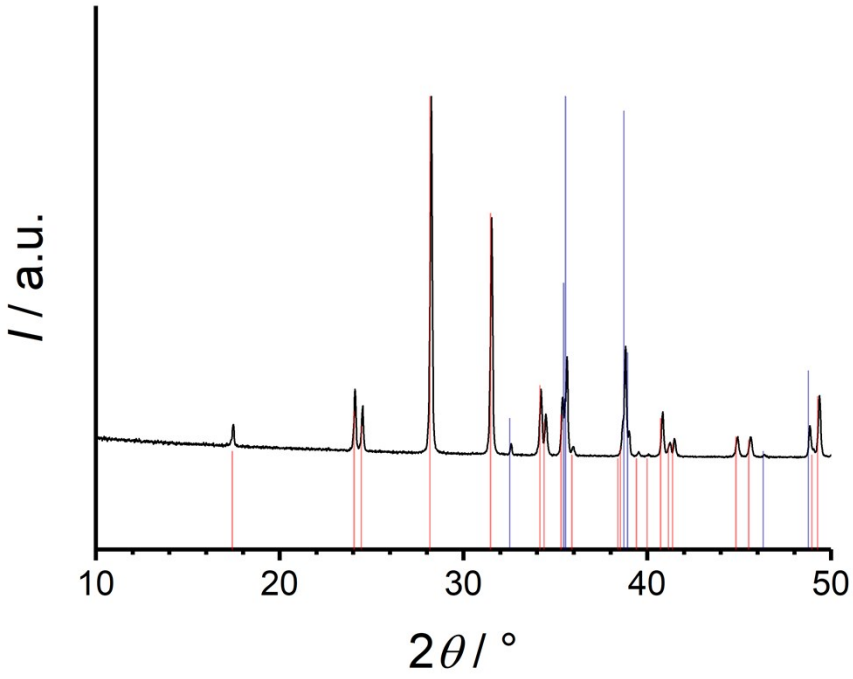

Figure S8: Powder XRD pattern of the residue after a thermogravimetric analysis of the MIL-140D-*sdc*/*abdc* sample prepared with 1 eq H_2*abdc* and 1 eq $CuCl_2$ 2 H_2O after the exposure to 100 ppm H_2S. The red lines represent the XRD pattern of ZrO_2 and the blue lines represent that of CuO.

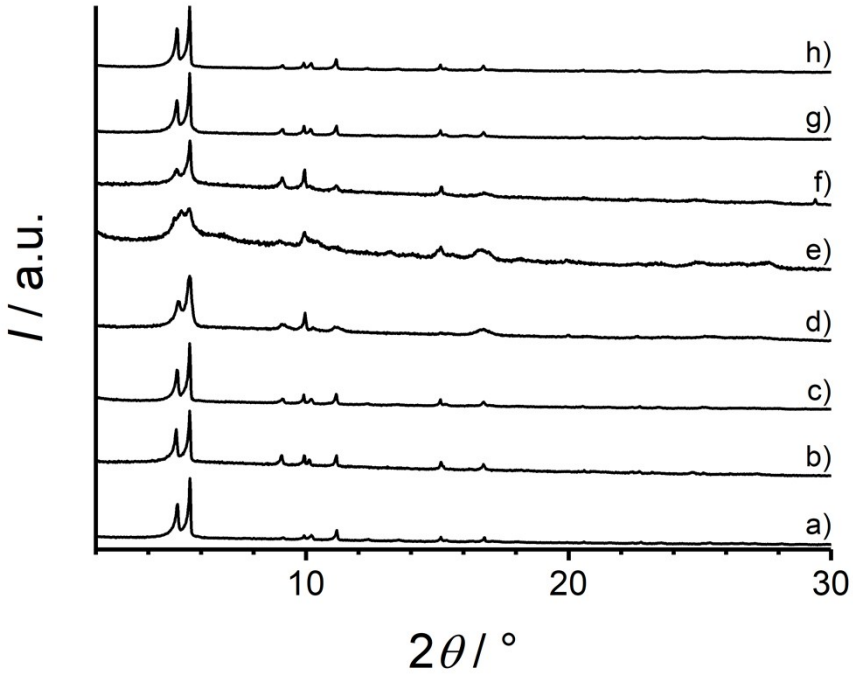

Figure S9: Powder XRD pattern of the MIL-140D-*sdc*/*abdc* sample prepared with 1 eq H_2*abdc* (a), after the incorporation of 1 eq $CuCl_2$ 2 H_2O (b) and after the exposure to different gases: c) H_2S (100 ppm), d) CO_2 (100 ppm), e) CO (100 ppm), f) NO_2 (10 ppm), g) NH_3 atmosphere, h) diethyl ether atmosphere.

IR and Raman spectroscopy

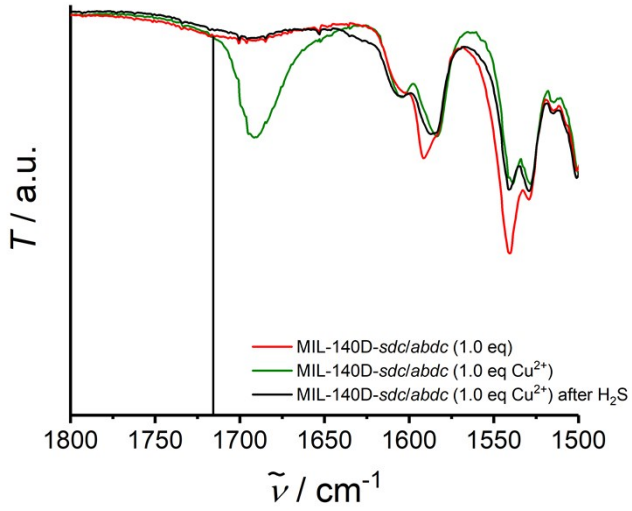

Figure S10: IR-spectra of the products of the SALE of MIL-140D-*sdc* with 1.0 eq H_2*abdc* (red), the sample after the incorporation of Cu^{2+} (green) and after the H_2S exposition (black). The black line indicates the usual position of the carbonyl vibration of acetone.

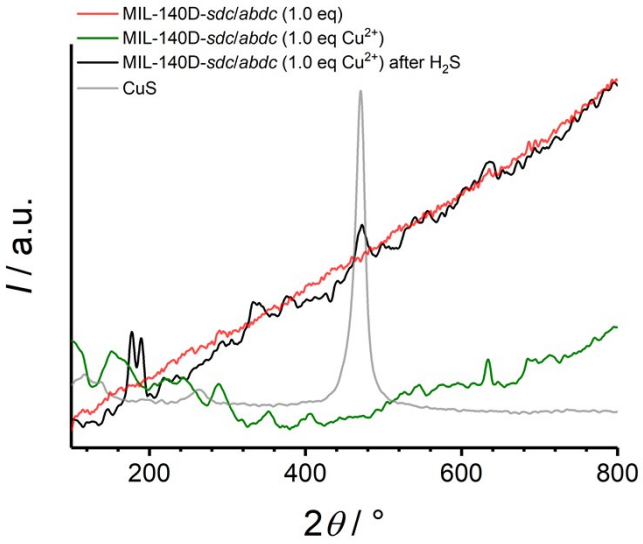

Figure S11: Raman-spectra of the products of the SALE of MIL-140D-*sdc* with 1.0 eq H_2*abdc* (red), the sample after the incorporation of Cu^{2+} (green), after the H_2S exposition (black) and pure CuS (grey).

Physisorption measurements

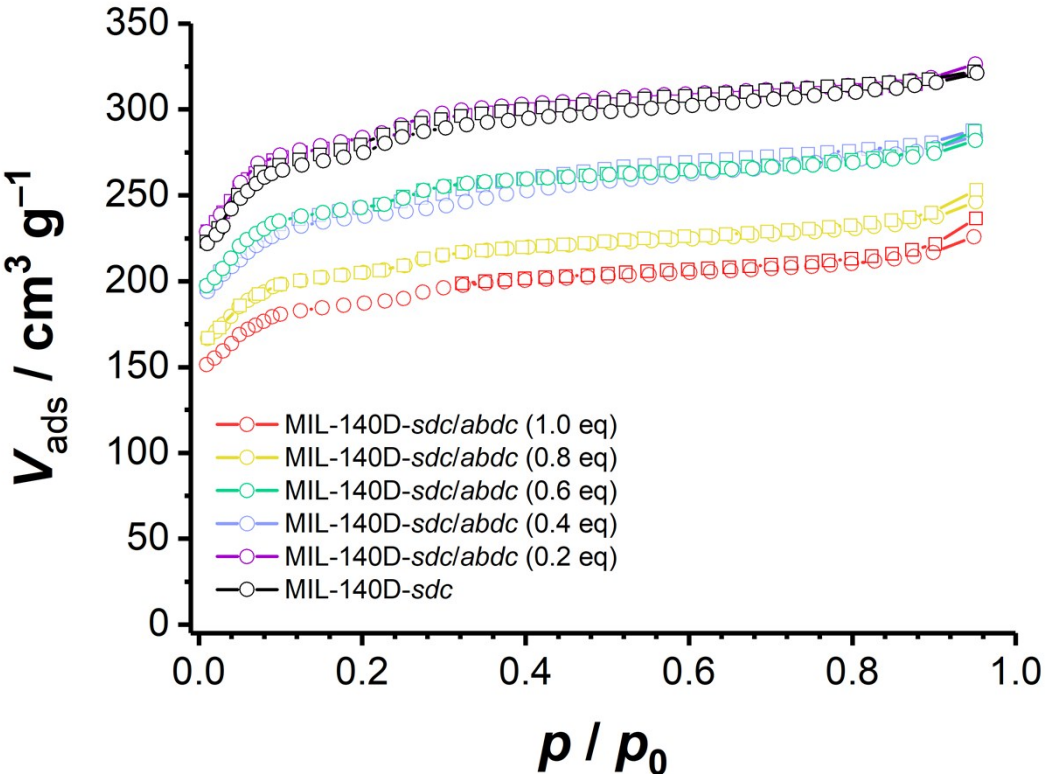

Figure S12: N_2 physisorption measurements of the products of the SALE of MIL-140D-*sdc* with 0.2 eq, 0.4 eq, 0.6 eq, 0.8 eq and 1.0 eq H_2*abdc* (purple, blue, green, yellow, red) and the starting material (black) at 77 K. The circles mark the measuring points of the adsorption and the squares those of the desorption.

Table S5: Calculated BET surface of N_2 physisorption measurements of MIL-140D-*sdc* and the MOFs prepared with SALE.

Amount of exchanged linker / eq	BET surface / m^2 g^{-1}
0.0 (MIL-140D-*sdc*)	1074
0.2	1097
0.4	1033
0.6	949
0.8	798
1.0	728

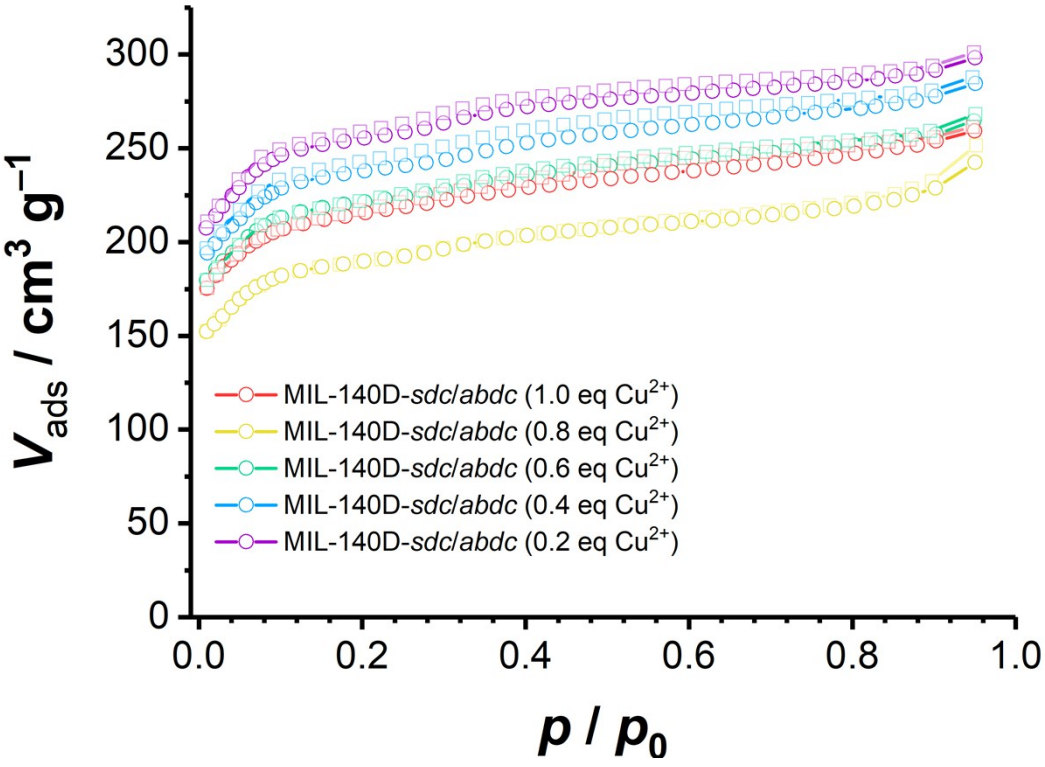

Figure S13: N_2 physisorption measurements of the products after the incorporation of Cu^{2+} into the samples of the SALE of MIL-140D-*sdc*/*abdc* with 0.2 eq, 0.4 eq, 0.6 eq, 0.8 eq and 1.0 eq H_2*abdc* (purple, blue, green, yellow, red) at 77 K. The circles mark the measuring points of the adsorption and the squares those of the desorption.

Table S6: Calculated BET surface of N_2 physisorption measurements of the Cu^{2+} incorporated MOFs prepared with SALE.

Amount of exchanged linker / eq	BET surface / m^2 g^{-1}
0.2	988
0.4	913
0.6	853
0.8	732
1.0	826

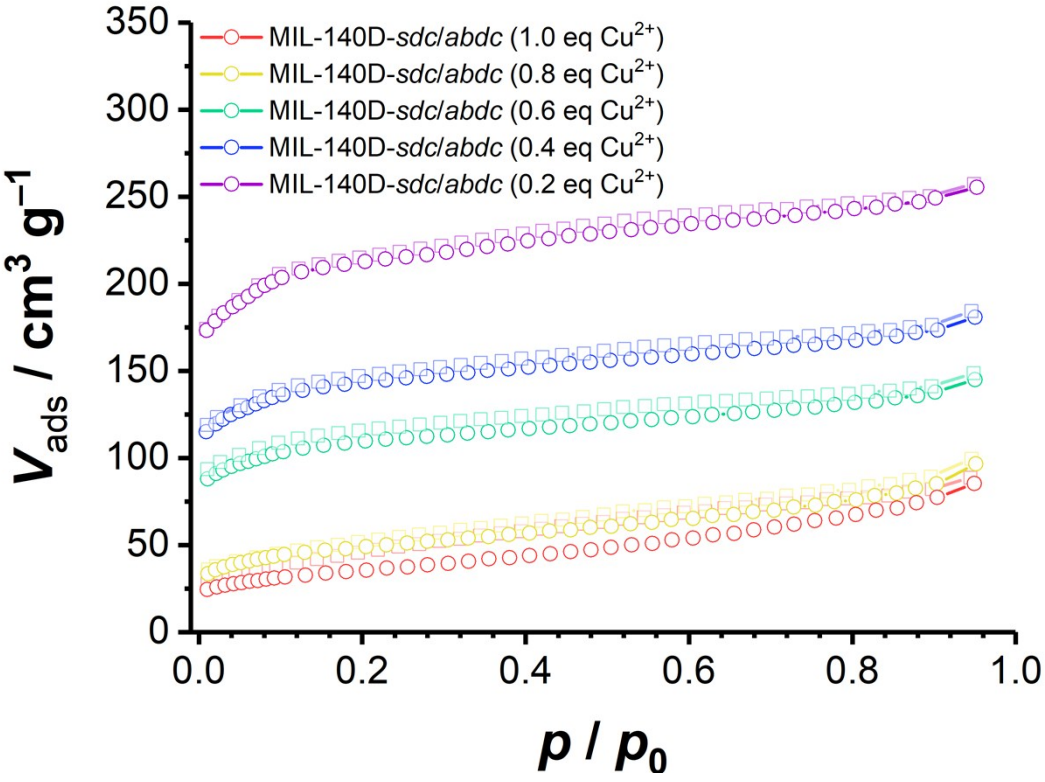

Figure S14: N_2 physisorption measurements of the products after the exposure to 100 ppm H_2S of Cu^{2+} incorporated MIL-140D-*sdc*/*abdc* with 0.2 eq, 0.4 eq, 0.6 eq, 0.8 eq and 1.0 eq H_2*abdc* (purple, blue, green, yellow, red) at 77 K. The circles mark the measuring points of the adsorption and the squares those of the desorption.

Table S7: Calculated BET surface of N_2 physisorption measurements after the exposure to 100 ppm H_2S.

Amount of exchanged linker / eq	BET surface / $m^2\ g^{-1}$
0.2	810
0.4	540
0.6	409
0.8	181
1.0	128

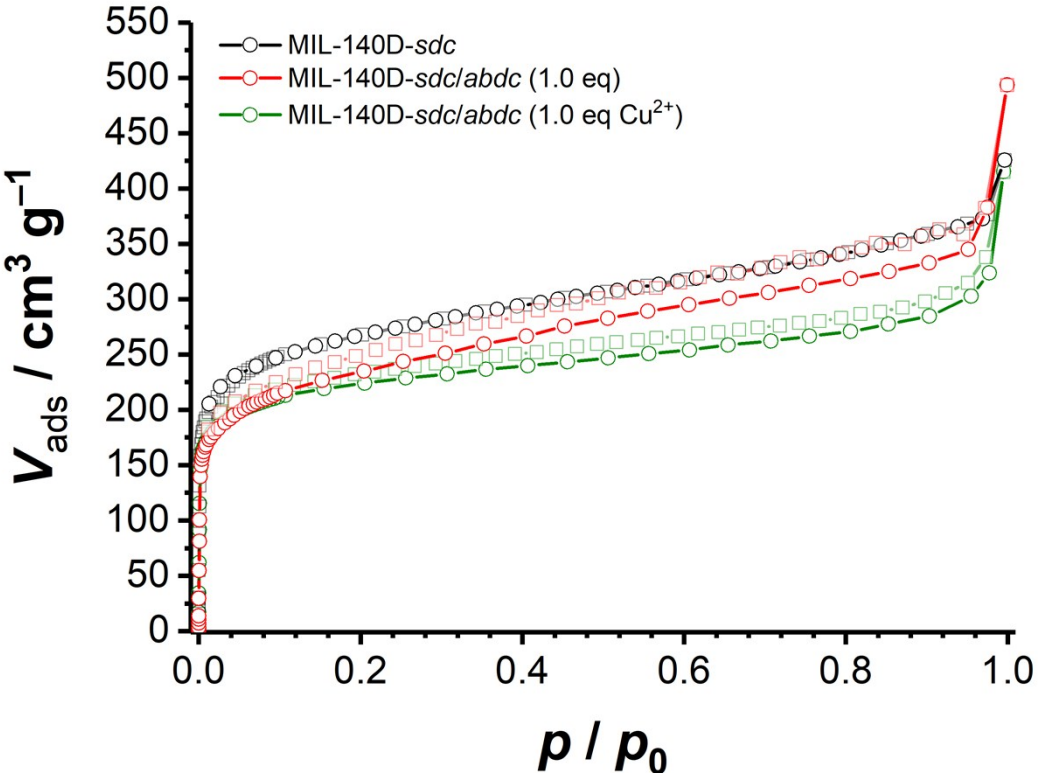

Figure S15: Ar physisorption measurements of the MIL-140D-*sdc* (black), the MIL-140D-*sdc*/*abdc* with 1 eq exchanged linker (red) and the Cu^{2+} incorporated MIL-140D-*sdc*/*abdc* with 1.0 eq H_2*abdc* (green) at 87 K. The circles mark the measuring points of the adsorption and the squares those of the desorption.

Table S8: Calculated BET surface of N_2 physisorption measurements after the exposure to 100 ppm H_2S.

Material	BET surface (Ar) / $m^2\ g^{-1}$
MIL-140D-*sdc*	810
MIL-140D-*sdc*/*abdc* (1 eq)	760
MIL-140D-*sdc*/*abdc* (Cu)	740

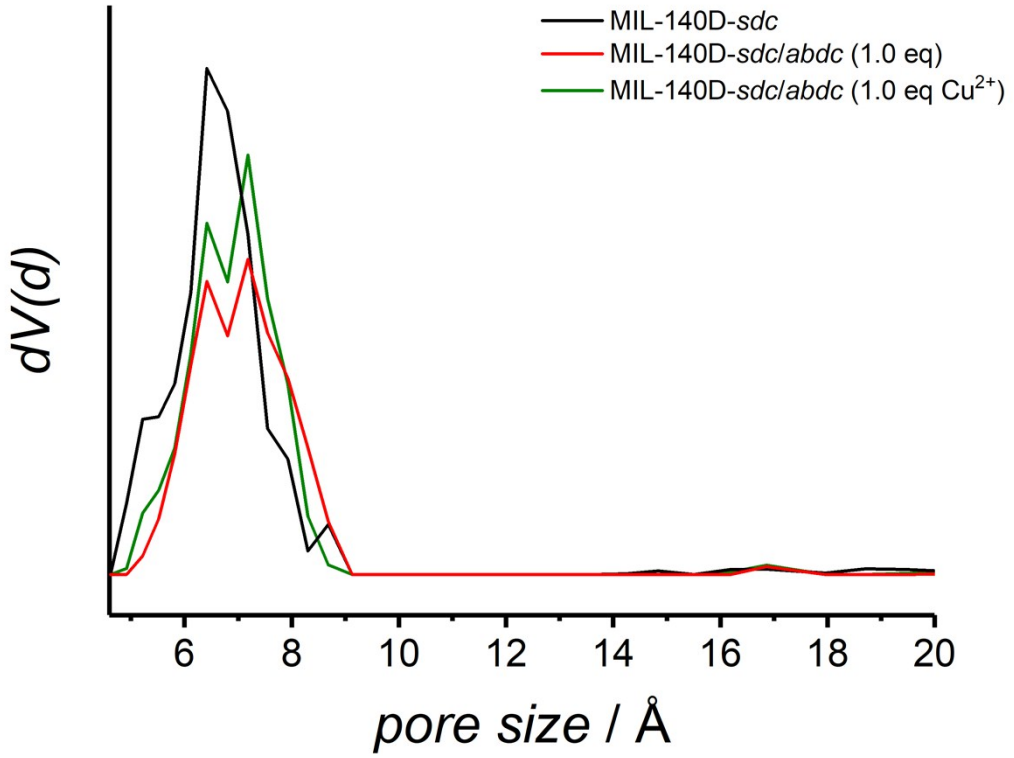

Figure S16: Pore size distribution of the MIL-140D-*sdc* (black), the MIL-140D-*sdc*/*abdc* with 1 eq exchanged linker (red) and the Cu^{2+} incorporated MIL-140D-*sdc*/*abdc* with 1.0 eq H_2*abdc* (green) at 87 K.

SEM investigation and EDXS

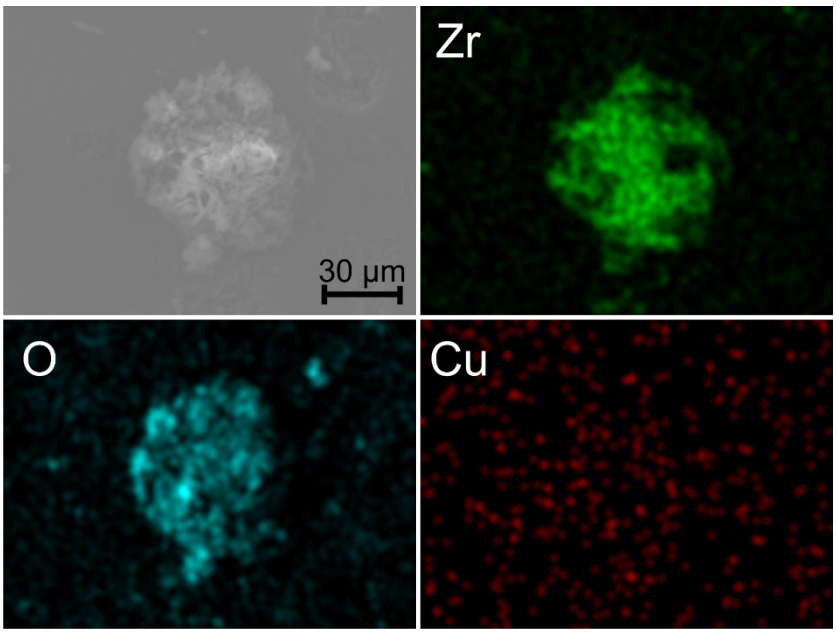

Figure S17: EDXS measurements of MIL-140D-*sdc*/*abdc* after the SALE with 1 eq H_2*abdc.*

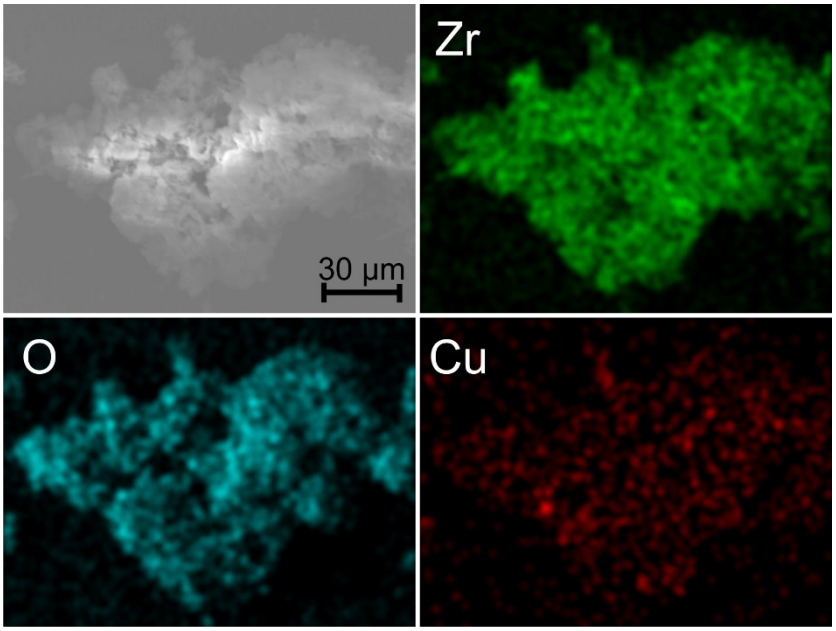

Figure S18: EDXS measurements of MIL-140D-*sdc*/*abdc* after the SALE with 1 eq H_2*abdc* and the incorporation of 0.5 eq $CuCl_2$ 2 H_2O (50%).

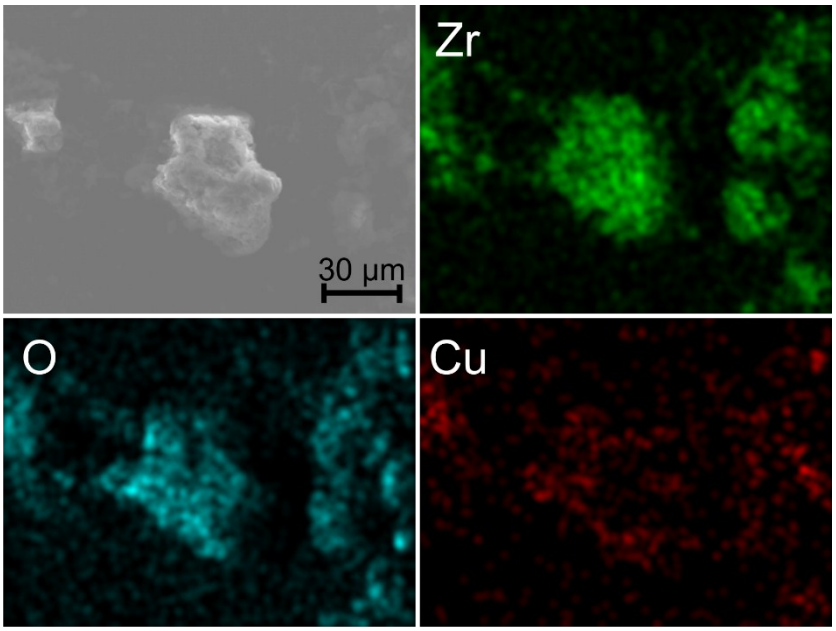

Figure S19: EDXS measurements of MIL-140D-*sdc*/*abdc* after the SALE with 1 eq H_2*abdc* and the incorporation of 1 eq $CuCl_2$ 2 H_2O (100%).

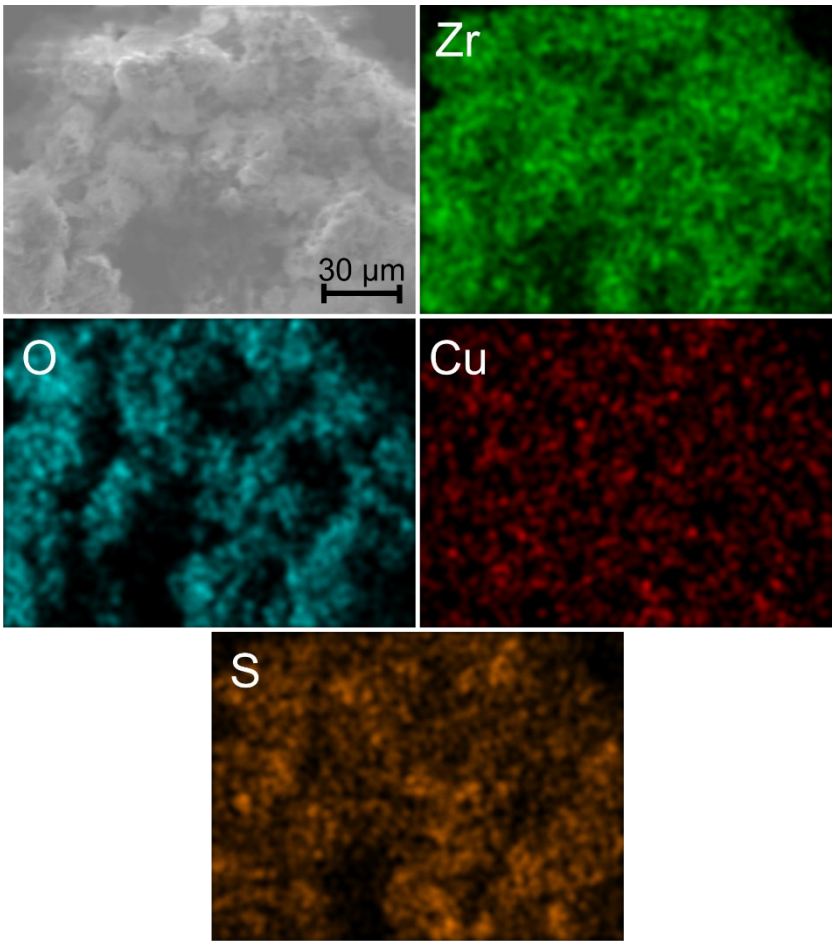

Figure S20: EDXS measurements of MIL-140D-*sdc*/*abdc* after the SALE with 1 eq H_2*abdc*, the incorporation of 0.5 eq $CuCl_2$ 2 H_2O and the exposure to 100 ppm H_2S.

Table S9: Result of the EDX measurements from the previous figures given in atomic percent plus error.

	Product of SALE / at.%	After 0.5 eq Cu^{2+} / at.%	After 1.0 eq Cu^{2+} / at.%	After H_2S / at.%
Zr	1.91 ± 0.49	2.10 ± 0.54	1.86 ± 0.40	2.81 ± 0.56
Cu	0.00 ± 0.04	0.88 ± 0.29	0.84 ± 0.40	1.37 ± 0.30
O	16.33 ± 3.17	19.01 ± 3.43	18.33 ± 4.04	20.09 ± 2.82
S	-	-	-	1.16 ± 0.11

Thermogravimetric measurement

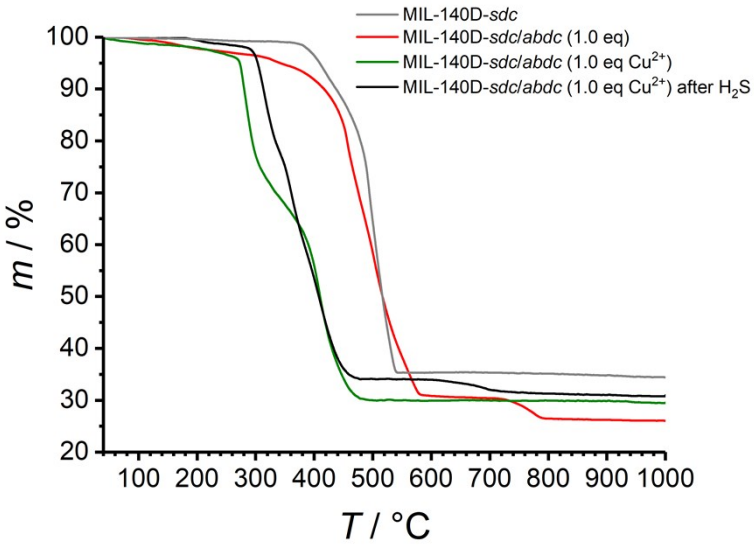

Figure S21: Thermogravimetric analysis of MIL-140D-*sdc* (grey) and of the products of the SALE of MIL-140D-*sdc* with 1.0 eq H_2*abdc* (red), after the incorporation of Cu^{2+} (green) and after the H_2S exposition (black). The samples were previously heated at 120°C to remove residual solvent molecules. The additional step at 700 °C can be explained by Zr^{4+} cations which are still coordinated by carboxylates after the linker decomposed at approximately 300 °C. At 700 °C these carboxylates are released and the transition to ZrO_2 takes place.[6]

Table S10: Comparison of calculated and experimental residues of the different MIL-140D-*sdc*/*abdc* samples.

	MIL-140D-*sdc*	Product of SALE	After Cu^{2+}	After H_2S
Experimental residue / *m*%	34.4	26.1	29.6	30.9
Without guest molecules / *m*%	34.9	27.0	31.5	31.6
Calculated residue / *m*%	33.0	33.0	33.0	33.0

UV/Vis measurement

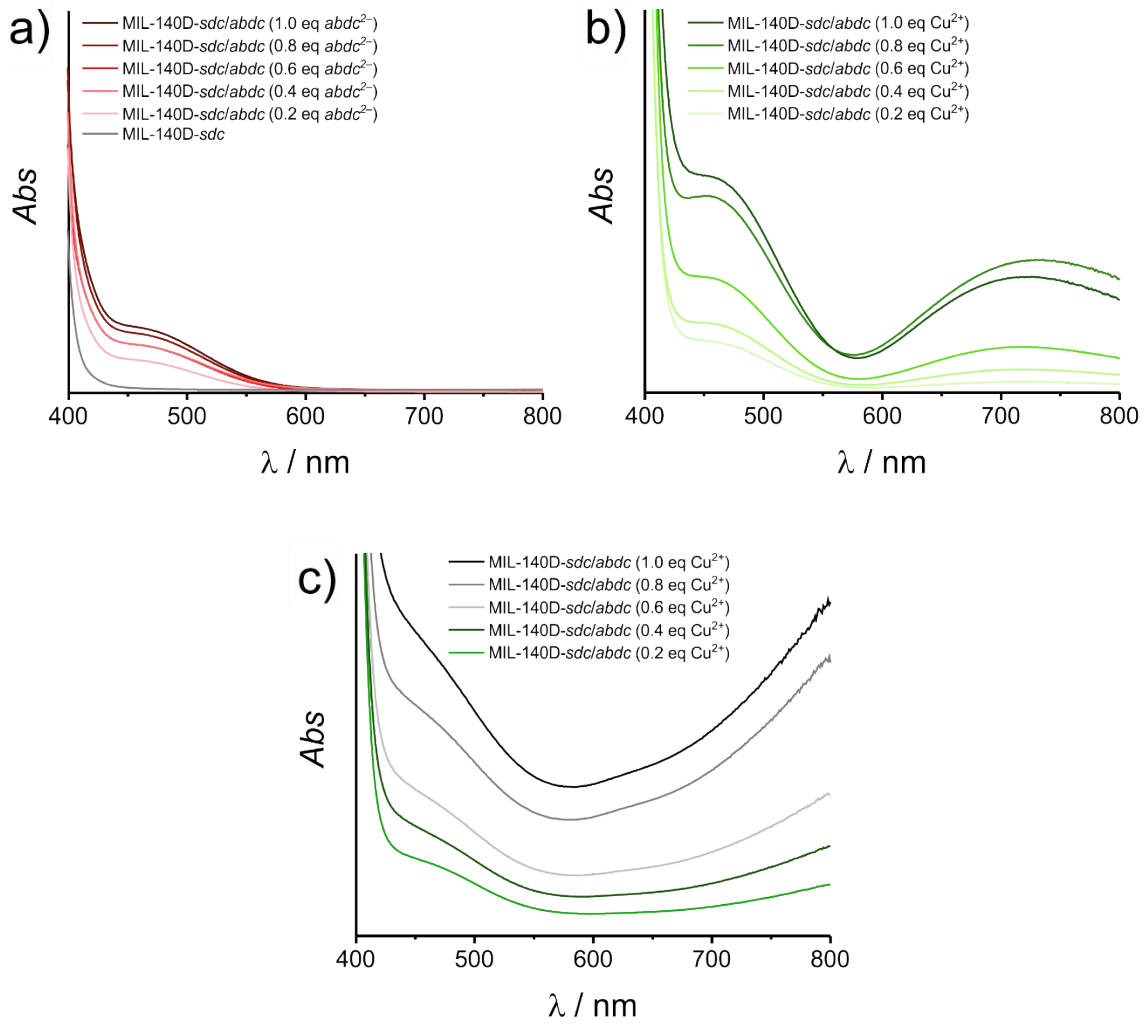

Figure S22: Measured UV/Vis spectra of the prepared MOF samples, from a) MIL-140D-*sdc* (grey) and the products after SALE (light red to dark red with increasing linker content), b) the copper incorporated samples (light green to dark green with increasing copper content), c) the samples after exposure of 100 ppm H_2S (green to black with increasing copper content).

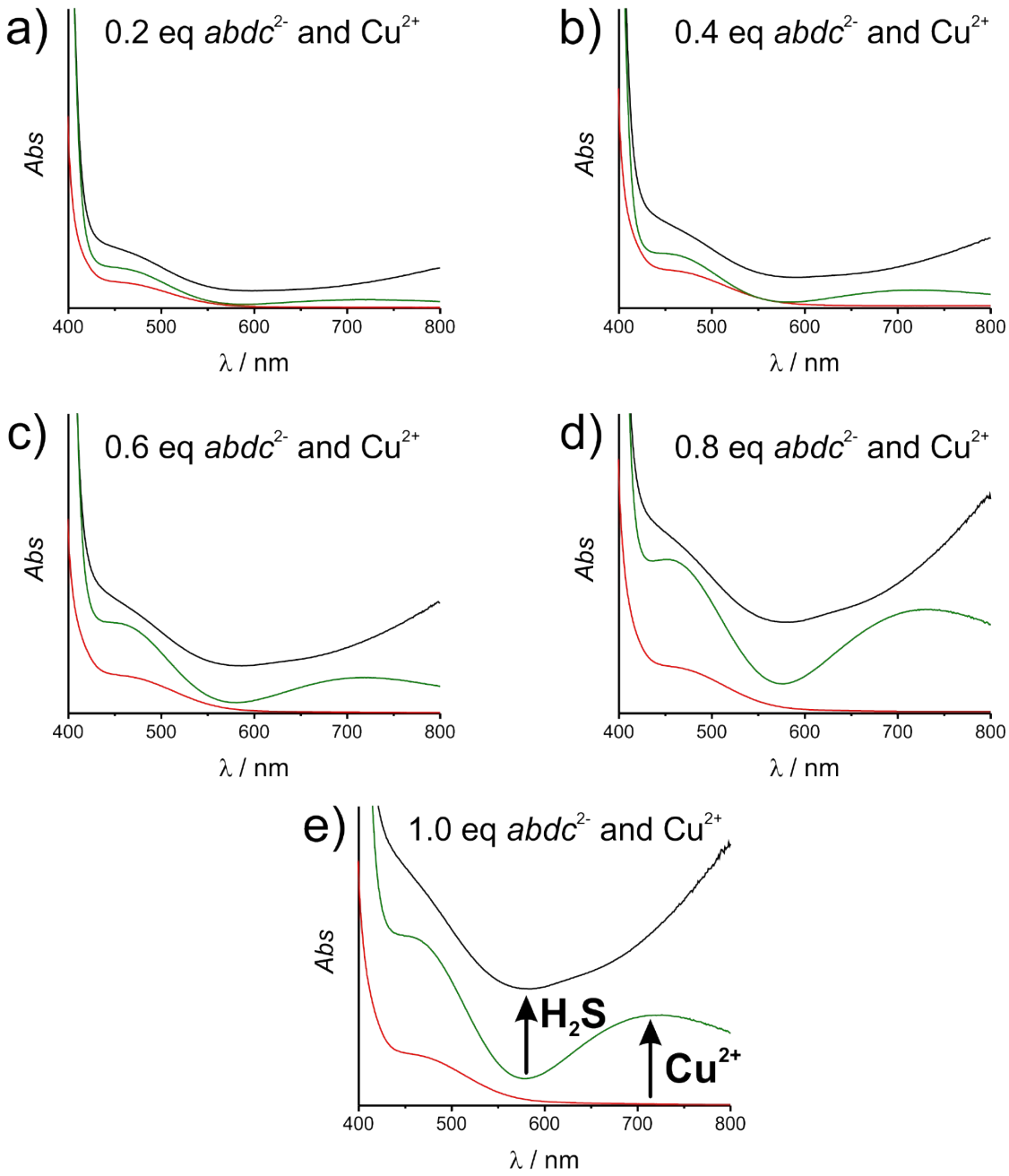

Figure S23: Measured UV/Vis spectra of individual MOF samples after the SALE (red), copper incorporation (green) and exposure of 100 ppm H_2S (black), with a) 0.2 eq, b) 0.4 eq, c) 0.6 eq, d) 0.8 eq and 1.0 eq H_2*abdc* and $CuCl_2$ 2 H_2O.

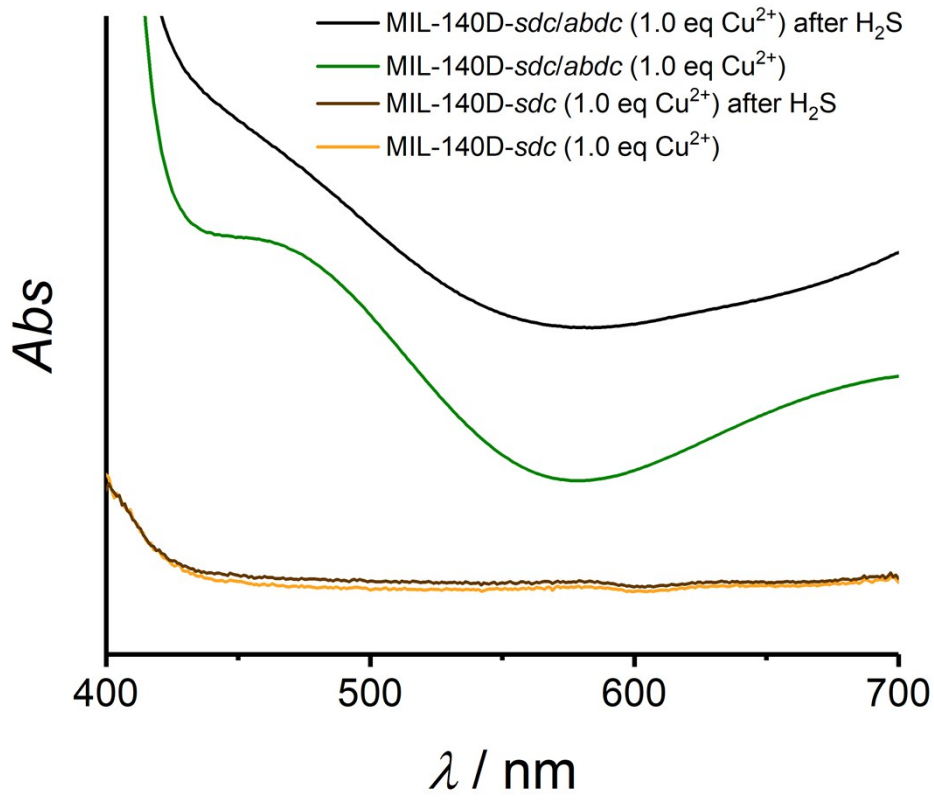

Figure S24: Measured UV/Vis spectra of the prepared MIL-140D-*sdc* after the incorporation of Cu^{2+} (yellow) and after exposure of 100 ppm H_2S (brown) and the corresponding sample of the *mixed-linker* MOF MIL-140D-*sdc*/*abdc* after copper incorporation (green) and after exposure of 100 ppm H_2S (black).

Figure S25: UV/Vis spectra of the MIL-140D-*sdc*/*abdc* sample prepared with 1.0 eq H_2*abdc* after incorporation of 1.0 eq $CuCl_2$ 2 H_2O and after the exposure to different gases: 50 ppm H_2S 100 ppm CO_2, 100 ppm CO, 10 ppm NO_2 and in NH_3 and diethyl ether atmosphere (from left to right).

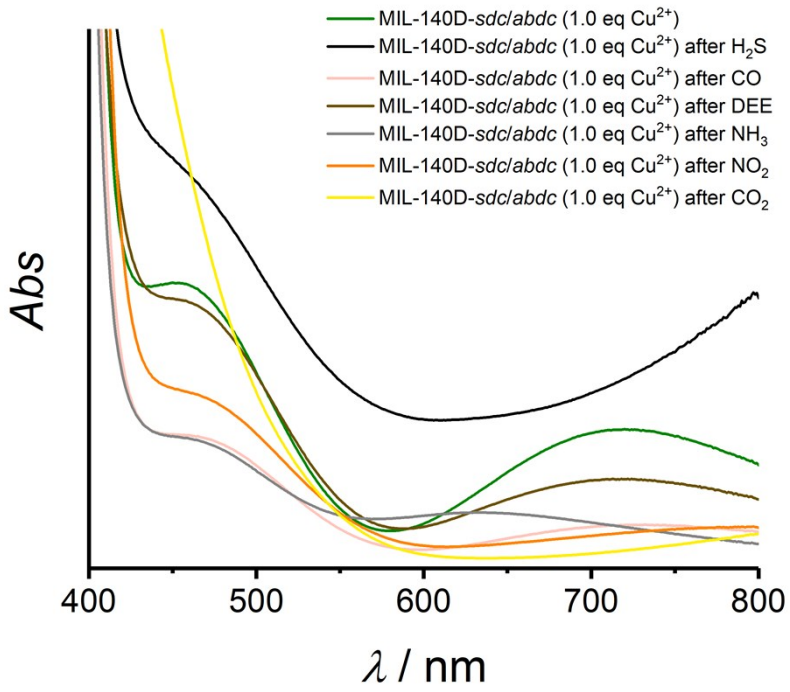

Figure S26: UV/Vis spectra of the MIL-140D-*sdc*/*abdc* sample prepared with 1.0 eq H_2*abdc* (red), after incorporation of 1.0 eq $CuCl_2$ 2 H_2O (green) and after the exposure to different gases: 50 ppm H_2S (black) 100 ppm CO_2 (yellow), 100 ppm CO (light red), 10 ppm NO_2 (orange), and in NH_3 and diethyl ether atmosphere (grey and brown).

References

1 C. C. Epley, M. D. Love and A. J. Morris, *Inorg. Chem.*, 2017, **56**, 13777–13784.

2 A. Schaate, S. Dühnen, G. Platz, S. Lilienthal, A. M. Schneider and P. Behrens, *Eur. J. Inorg. Chem.*, 2012, **2012**, 790–796.

3 L. Engel, K. R. Tarantik, C. Pannek and J. Wöllenstein, *Sensors*, 2019, **19**, DOI: 10.3390/s19051182.

4 M. Schulz, N. Marquardt, M. Schäfer, D. P. Warwas, S. Zailskas and A. Schaate, *Chem. Eur. J.*, 2019, **25**, 13598–13608.

5 V. Guillerm, F. Ragon, M. Dan-Hardi, T. Devic, M. Vishnuvarthan, B. Campo, A. Vimont, G. Clet, Q. Yang, G. Maurin, G. Férey, A. Vittadini, S. Gross and C. Serre, *Angew. Chem. Int. Ed.*, 2012, **51**, 9267–9271.

6 G. Wißmann, A. Schaate, S. Lilienthal, I. Bremer, A. M. Schneider and P. Behrens, *Microporous Mesoporous Mat.*, 2012, **152**, 64–70.